2. PROCESSES OF FA AND DDT*

2.1 Introduction

A freely expanding flame is intrinsically unstable. It has been demonstrated, both in laboratory-scale experiments [2.1-2.4] and large-scale experiments [2.5-2.8], that obstacles located along the path of an expanding flame can cause rapid flame acceleration. Qualitatively, the mechanism for this flame acceleration is well understood. Thermal expansion of the hot combustion products produces movement in the unburned gas. If obstacles are present, turbulence can be generated in the combustion-induced flow. Turbulence increases the local burning rate by increasing both the surface area of the flame and the transport of local mass and energy. An overall higher burning rate, in turn, produces a higher flow velocity in the unburned gas. This feedback loop results in a continuous acceleration of the propagating flame. Under appropriate conditions, this can lead to transition to detonation.

Turbulence induced by obstacles in the displacement flow does not always enhance the burning rate. Depending on the mixture sensitivity, high-intensity turbulence can lower the overall burning rate by excessive flame stretching and by rapid mixing of the burned products and the cold unburned mixture. If the temperature of the reaction zone is lowered to a level that can no longer sustain continuous propagation of the flame, a flame can be extinguished locally. The quenching by turbulence becomes more significant as the velocity of the unburned gas increases. For some insensitive mixtures, this can set a limit to the positive feedback mechanism and, in some cases, lead to the total extinction of the flame. Hence both the rate of flame acceleration and the eventual outcome (maximum flame speed attained) depend on the competing effects of turbulence on combustion.

This chapter summarizes some of the key findings since the publishing of the last state-of-the-art report on DDT in 1991. It should be noted that to give a comprehensive discussion of the phenomena on flame acceleration and DDT is beyond of the scope of this chapter. Only a brief overview of recent works is presented. Furthermore, this chapter only cites studies that are relevant to the nuclear industry.

To provide a proper perspective of the issue, this chapter describes in some detail the key mechanisms that are responsible for flame acceleration and transition to detonation. It outlines the various eventual outcomes of flame acceleration. It also summarizes some of the recent studies that have contributed to the current understanding of the phenomena. Finally, this chapter discusses the various possible responses of a structure that has been subjected to a pressure load resulting from an accelerated flame or a detonation wave.

2.2 Flame and Detonation Propagation Regimes

Depending on the fuel concentration and the flow geometry, flame acceleration may be expected to progress through a series of regimes, as depicted in Figure 2.2-1. For the case of mild ignition, the first phase involves a laminar flame that propagates at a velocity determined by the laminar burning velocity and the density ratio across the flame front. This phase of the flame propagation is very well understood, and data are available for a wide range of hydrogen-air mixtures. The laminar flame propagation regime is relatively short-lived and is soon replaced by a "wrinkled" flame regime. For

* Lead authors of Chapter 2 are Dr. Calvin Chan of AECL and Dr. Paul Thibault of Combustion Dynamics Ltd.

most accidental explosions, this regime can persist over relatively large flame propagation distances. For this reason, it is therefore far more important than the initial laminar regime. Because of the increase in flame area, the burning rate, and hence the flame propagation velocity for the wrinkled flame can be several times higher than for the laminar flame.

Because of turbulence generated by obstacles or boundary layers, the wrinkled flame eventually transforms into a turbulent flame brush. This change results in further flame acceleration because of the increase in surface area of the laminar flamelets inside the flame brush. For sufficiently high levels of turbulence, the flamelet structure may be destroyed and then replaced by a distributed reaction zone structure.

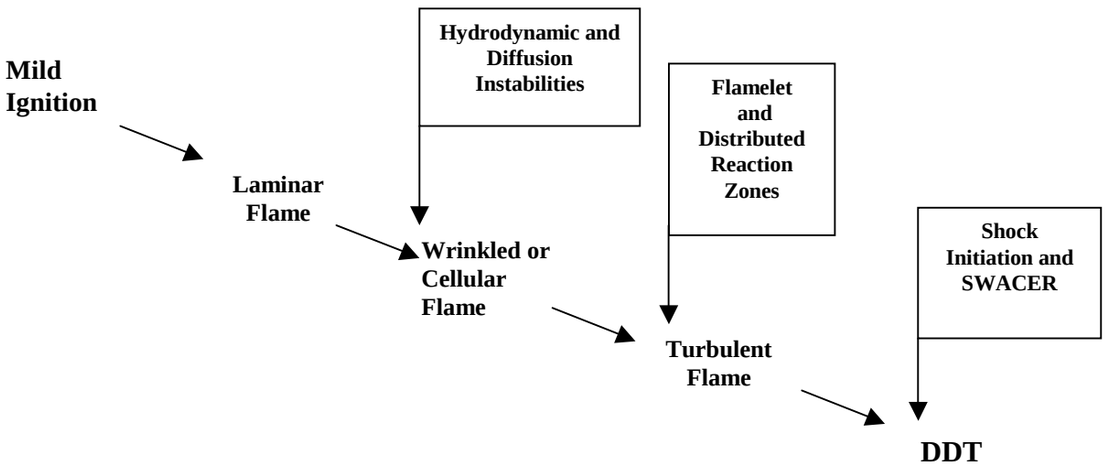

Figure 2.2-1 Regimes of flame propagation leading to DDT
(SWACER = shock wave amplification by coherent energy release)

The flame acceleration process can eventually lead to DDT through shock ignition or the SWACER amplification mechanism. For configurations involving repeated obstacles, the turbulent flame propagation regime is self-accelerating because of the feedback mechanism between the flame velocity and the level of turbulence ahead of the flame front. The final flame velocity produced by the turbulent flame acceleration process depends on a variety of parameters, including the mixture composition, the dimensions of the enclosure, and the size, shape, and distribution of the obstacles.

Figure 2.2-2 shows the flame trajectories for flame propagation in tubes filled with obstacles. Figure 2.2-3 shows the maximum flame speed achievable in tubes of various diameters. Various turbulent flame and detonation propagation regimes have been identified for hydrogen-air mixtures in obstacle-filled tubes. These regimes include

1. a quenching regime where the flame fails to propagate,

2. a subsonic regime where the flame is travelling at a speed that is slower than the sound speed of the combustion products,

3. a choked regime where the flame speed is comparable with the sound speed of the combustion products,

4. a quasi-detonation regime with a velocity between the sonic and Chapman-Jouguet (CJ) velocity,

5. a CJ detonation regime where the propagation velocity is equal to the CJ detonation velocity.

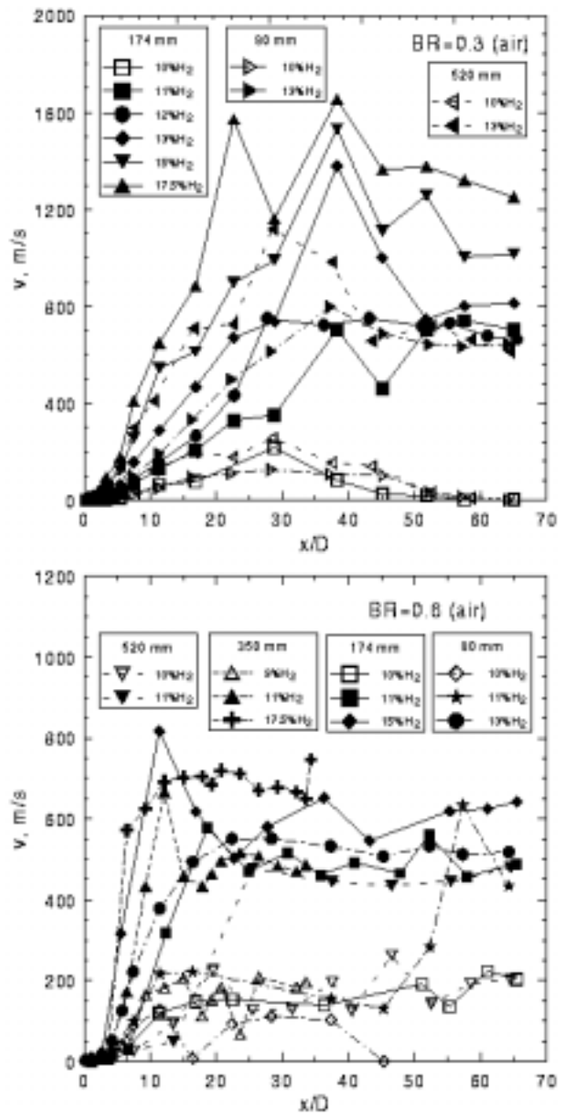

Figure 2.2-2. Visible speeds of turbulent flame propagation versus reduced distance along tubes (D - tube diameter) for lean hydrogen-air mixtures. Blockage Ratio (BR) = 0.3 (upper) and 0.6 (lower). Obstacle spacing is equal to D. Solid points - fast combustion regimes (choked flames and quasi-detonations), empty points - slow combustion regimes [2.9].

It should be noted that the above regimes are geometry-dependent for a given mixture. Consequently, the concentration range for each regime in Figure 2.2-3 may differ for circular tubes and rectangular channels.

2.2.1 Quenching Regime

For sufficiently large BRs (blocked area and total cross-sectional area) in which the pressure difference across the orifice plate can build up rapidly, the flame is observed first to accelerate and then to quench itself after propagating past a certain number of orifice plates. This regime is referred to as the "quenching regime". (Quenching means that the flame ultimately ceases to propagate.) In this regime, flame propagation can be considered as the successive explosion of a continuous sequence of combustion chambers interconnected by orifice plates. Ignition of the mixture in one chamber is achieved by the venting of the hot combustion products from the upstream chamber through the orifice. Quenching occurs when the hot turbulent jet of product gases fails to cause ignition in the downstream chamber because of the rapid entrainment and turbulent mixing of the cold unburned mixture with the hot product of the jet. As shown in Figure 2.2-3, for most hydrogen-air mixtures, the boundaries between the quenching regime and the other flame propagation regimes are very distinct.

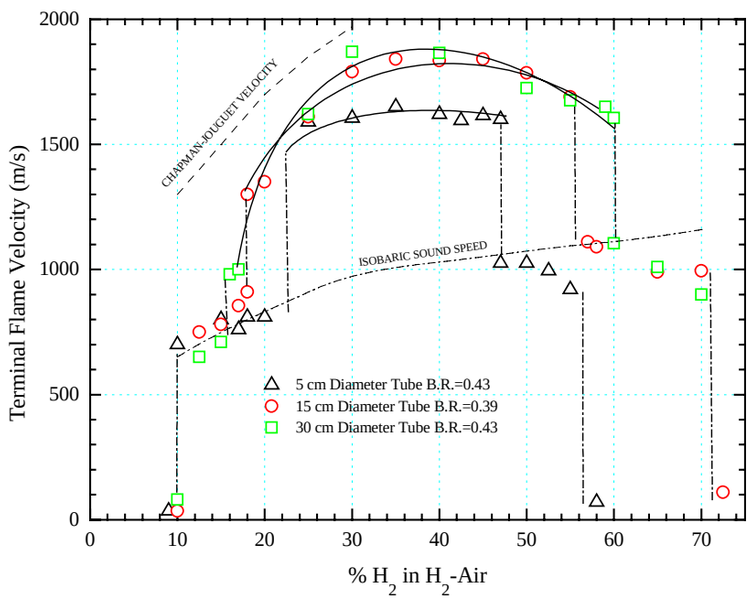

Figure 2.2-3. Maximum flame speeds for H_2-air mixtures in tubes of different sizes

2.2.2 Subsonic Flame Regime

Total quenching of hydrogen-air flames is not always possible. In this case, a quasi-steady flame with an average velocity range from a few tens of metres per second to a couple hundreds of metres per second is possible. This subsonic velocity is a result of a competition of the positive (enhancement)

and the negative (quenching) aspects of turbulence on combustion. Such a flame is highly unstable. A slight change in the boundary condition can cause the flame to quench totally or suddenly jump to another flame propagation regime. This instability is clearly shown in Figure 2.2-3.

2.2.3 Choking Regime

When the conditions for quenching are not met, the flame continuously accelerates to reach a final steady-state value. When this happens, flame propagation can be considered as a quasi-steady one-dimensional compressible flow in a pipe with friction and heat addition. This regime is referred to as the choking regime, where the combined effects of wall friction and heat addition control the final steady-state flame speed.

2.2.4 Quasi-detonation Regime

Since the flame speeds typically attained in the choking regime are of the order of 1000 m/s, a local explosion leading to an onset of detonation may occur. If the orifice diameter, d, is sufficiently large, a stable detonation wave can be formed. For detonation combustion, it is found that the detonation cell size, λ, provides an important characteristic length that can be used to determine the limit of detonation propagation. When d/λ exceeds a certain critical value, a successful transition from deflagration to detonation can occur. In the detonation regime, the propagation mechanism will be one of shock ignition and transverse wave motion corresponding to a normal detonation. The detonation velocity, however, can be significantly below that of the normal CJ value because of the severe momentum losses in the obstacle-filled tube. In previous studies of detonation propagation in very rough tubes by Shchelkin [2.10] and Guenoche and Manson [2.11], detonation velocities of less than 50% of the CJ value have been observed. Such sub-CJ steady-state detonation waves have been called quasi-detonation waves. As a result, this regime is referred to as the "quasi-detonation regime".

2.2.5 CJ Detonation Regime

To examine flame propagation in tubes of different sizes, similar experiments were performed with various hydrogen-air mixture in three different tubes. Results are summarized in Figure 2.2-3. The above propagation regimes are clearly visible. It is of interest to note that in a composition of near 24% H_2-air there occurs another transition within the detonation regime itself. In this case the transition is from the sub-CJ quasi-detonation regime discussed above to the CJ detonation regime. The cell size for the 24% H_2-air composition is about 2 cm. This gives a value of $d/\lambda = 13$, which is the condition at which the detonation propagation would be insensitive to the wall effects. That is to say, if the unobstructed area in a tube is sufficiently large, the propagation of a detonation wave is unaffected by the obstruction.

2.2.6 Criteria for the Various Propagation Regimes

As seen from Figure 2.2-3, an increase in the tube diameter results in an increase in the threshold concentrations for the transition between the various regimes. Various criteria have been proposed for these transitions. Requirements for fast and unstable flames may be expressed in terms of a criteria, described in Section 3.2.2, which is expressed in terms of the combustion expansion ratio, the flame thickness, and a geometric scale. For the quenching regime, the minimum blockage diameter depends on the sensitivity of the mixture and the pressure gradient across the blockage during the passage of the flame front [2.12, 2.13]. For the quasi-detonation and CJ regimes, the criteria are usually

expressed in terms of a characteristic dimension such as the blockage or tube diameter, and the detonation cell size. A general guideline is that quasi-detonations become possible when the blockage diameter is larger than the detonation cell size, λ, for the mixture. A CJ detonation, on the other hand, is possible when the unobstructed tube diameter is larger than approximately 13λ, which corresponds to the critical tube diameter discussed in Section 2.3.2. For a particular obstacle geometry, the limiting conditions for DDT may also be described in terms of a 7λ criteria, which is described in Section 3.2 of this report.

2.3 The Effect of Confinement on Flame and Detonation Propagation

The limiting conditions for DDT discussed in the previous section represent the best currently available estimates of the necessary conditions. For DDT to occur, a flame needs to accelerate to beyond a certain critical flame speed. This speed is usually close to the choking flame speed (i.e., approximately 600 m/s). As a result, to assess the likelihood of DDT, it is necessary to examine the conditions that can affect the FA process. Examples of such conditions are the obstacle configuration (spacing and blockage) and the level of confinement of the surrounding walls.

2.3.1 Effect of Confinement on Flame Propagation

The positive feedback between the flame propagation and turbulence generation in a channel is very sensitive to the level of confinement in the channel [2.14-2.17]. A decrease in confinement, using top-venting, for example, reduces the flow velocity ahead of the flame, thereby reducing the obstacle-induced turbulence.

Large-scale experiments, with H_2-air mixtures relevant for reactor safety were performed in the FLAME facility [2.17]. FLAME is a large rectangular channel 30.5 m long, 2.44 m high, and 1.83 m wide. It is closed on the ignition end and open on the far end. The presence of the obstacles tested greatly increased the flame speeds, overpressures, and tendency for DDT compared with similar tests without obstacles. Similarly, transverse venting reduced the flame speeds, overpressures, and the possibility of DDT.

Figure 2.3.1-1 shows the maximum equivalent planar flame speed as a function of hydrogen mole fraction for five series of tests, no top venting and no obstacles, 50% top venting and obstacles, and 13% top venting with no obstacles. Tests with no top venting are indicated with shaded squares; tests with 13% top venting are indicated with open triangles, and tests with 50% top venting are indicated with shaded circles. The tests with obstacles are distinguished from those without obstacles (dashed line instead of a solid line). For those tests in which DDT did occur, an upward pointing arrow from the maximum equivalent planar flame speed point indicates that the combustion accelerates and approaches detonation speeds.

The effect of the presence of obstacles is shown by the lower hydrogen concentration required to attain the same maximum equivalent flame speed or overpressure compared with a similar test without obstacles. With 50% top venting and no obstacles present, this speed would not have been attained even for a stoichiometric mixture. The inhibiting effect of large degrees of transverse venting on the flame speed and overpressures is evident. The complex behaviour of small degrees of transverse venting is observed in the 13% top venting test series. For lean mixtures below approximately 18% hydrogen mole fraction, the flame speeds are lower and overpressures comparable to those obtained in similar

tests without transverse venting. Above this hydrogen concentration, the flame speeds and overpressures are higher than in tests without transverse venting.

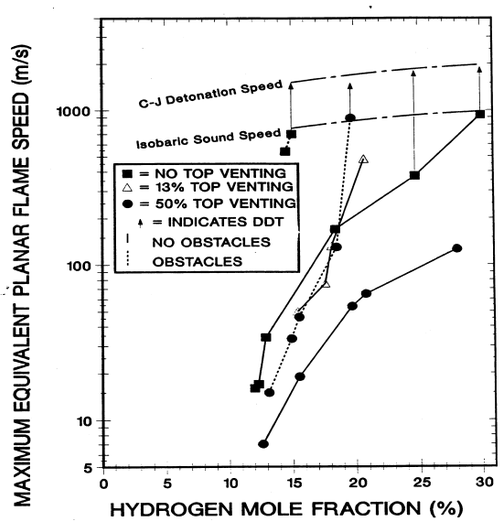

Figure 2.3.1-1 Combustion front velocity versus hydrogen mole fraction for hydrogen-air mixtures at 500 K and 0.1 MPa at the High-Temperature Combustion Facility at BNL. Open circles denote the average velocity over roughly the second half of the vessel and error bars represent the standard deviation in the measured velocity. Open squares denote the maximum flame velocity for slow deflagration.

2.3.2 Effect of Confinement on Detonation Propagation

As in the case of flames, detonations are also very sensitive to the level of confinement. A sudden removal of confinement at the end of a tube, for example, can result in detonation failure. The 'critical tube' diameter for which detonation failure occurs is determined by the sensitivity of the mixture, which is expressed in terms of the detonation cell size λ. For fuel-air mixtures with an irregular cellular structure, the critical diameter $D_c \cong 13\lambda$.

Figure 2.3.2-1 displays the detonation cell size data for a hydrogen-air mixture as a function of initial temperature [2.18, 2.19]. As seen from this figure for an initial temperature of 300 K, cell size measurements can vary by a factor of 2. This is due to differences in the interpretation and preparation of the smoke foils used to record the cellular structure.

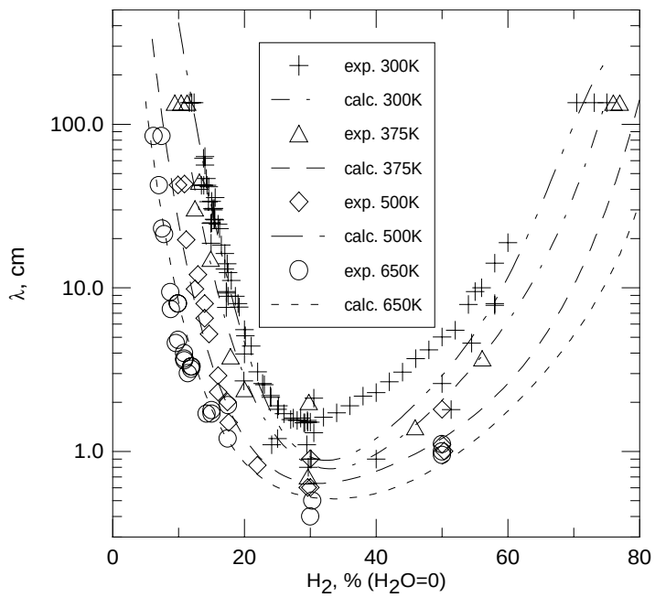

Figure 2.3.2-1 Detonation cell size for hydrogen-air mixture at different initial temperatures [2.18, 2.19]

2.4 Mechanisms Involved in FA

Although the various flame and detonation propagation regimes are relatively well established, the underlying mechanisms can be complex and, in some cases, poorly understood.

2.4.1 Laminar Flame and Flame-folding Regimes

The early stage of flame propagation involves a laminar flame regime followed by a wrinkled or cellular flame. The laminar flame velocity is determined by thermal and mass transport across the flame front and the heat released because of combustion. It can be predicted using readily available chemical kinetics codes. The more important wrinkled flame regime is controlled by a variety of diffusion and hydrodynamic instabilities that are much more difficult to model. The cellular flame propagation has been described by Markstein and Somers [2.20] and by Markstein [2.21] and theoretically analyzed by numerous authors, including Clavin and Williams [2.22], Joulin and Clavin [2.23], Pecle and Clavens [2.24]. The flame cell size typically varies between 0.5 cm and 3.5 cm and increases with the square of the burning velocity. Figure 2.4.1-1 displays typical flame structures as a function of the Lewis and Zel'dovich numbers [2.25]. A detailed view of the flame structure is also provided in Figure 2.4.1-2, which displays a laser-induced predissociation fluorescence (LIPF) image of a cellular flame front [2.26, 2.27]. From a modelling point of view, the flame-folding regime is usually addressed by adopting a flame surface enhancement factor that is derived from flame propagation experiments for a particular mixture composition.

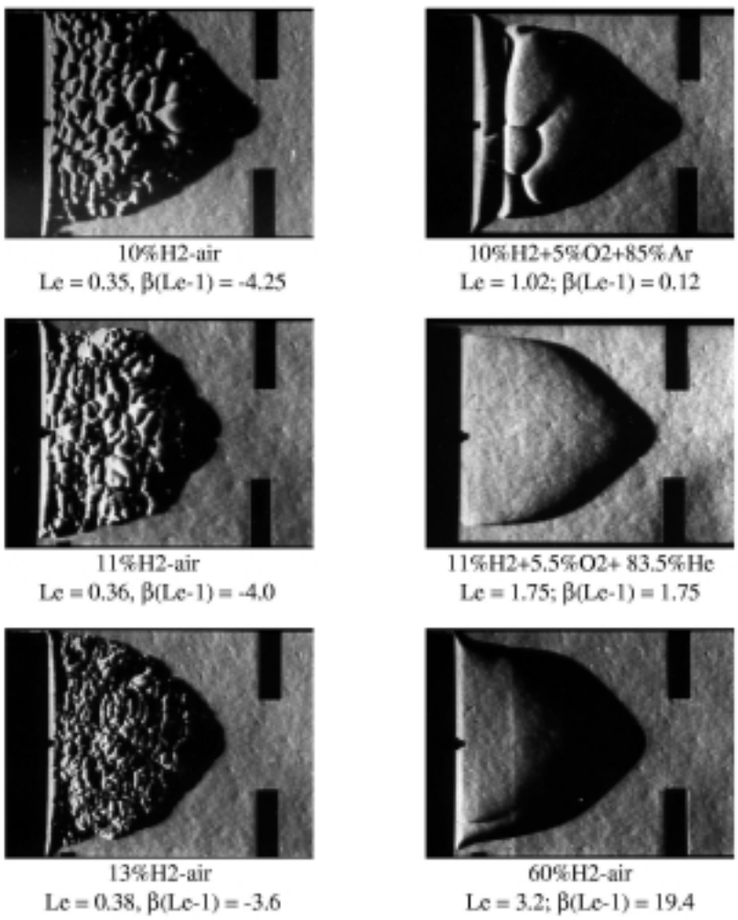

Figure 2.4.1-1 Effect of Lewis number on flame structure. Threshold for thermal-diffusion instability corresponds to $\beta(Le - 1) < -2$. $\beta = E_a(T_b-T_u)/T_b^2$ is Zel'dovich number, where E_a effective activation energy, T_u and T_b – unburned and burned gas temperatures [2.25].

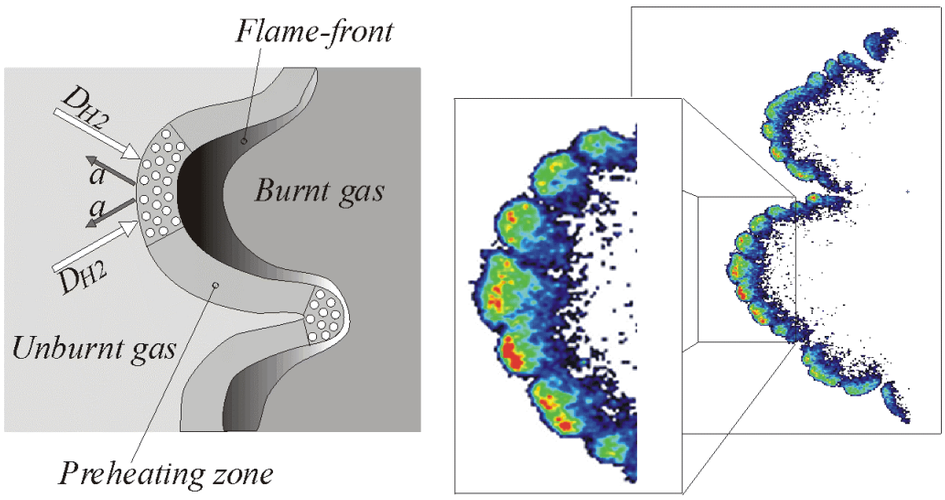

Figure 2.4.1-2 Schematic (left) illustrating competition between thermal diffusion, a, and hydrogen diffusion, $D_{H2,}$ in a lean hydrogen-air flame laser-induced predissociation fluorescence (LIPF) image (right) displaying reaction zone in cellular flame front [2.26, 2.27].

2.4.2 Turbulent Combustion and Acceleration

The wrinkled flame regime is soon followed by a turbulent flame regime when the flame encounters a wall or an obstacle. The mechanisms responsible for the turbulence include Kelvin-Helmholtz, or Rayleigh-Taylor instabilities, which are triggered when the flame is suddenly accelerated over an obstacle or through a vent [2.28]. In the case of a flame propagating over repeated obstacles, this is a self-accelerating process that is due to the feedback mechanism between the flame propagation and the flow velocity and turbulence generated ahead of the flame.

The structure of the turbulent flame brush depends greatly on the turbulence intensity and the characteristic time scales for combustion and turbulence. If the combustion time scale is smaller than the turbulent eddy turnover time, the flame brush may be modelled as consisting of a large number of distinct laminar "flamelets". On the other hand, if the combustion is slow compared with the eddy turnover time, the reaction zones inside the flame brush become distributed and require a different modelling approach. The Borghi diagram [2.29] provides a useful classification of turbulent combustion regimes based on non-dimensional numbers such as the Karlovitz and Damköhler numbers. Figure 2.4.2-1 displays a Borghi diagram with LIPF images of the flame structure for the various regimes [2.26]. As discussed in Chapter 4, the validity of theoretical models depends greatly on the Borghi diagram regime and the corresponding flame front structure.

2.4.3 Acoustic-flame and Shock-flame Interactions

Flame propagation in an enclosure generates acoustic waves that can interact with the flame front and promote flame acceleration though a variety of instability mechanisms. Such instabilities have been observed by Guenoche [2.30] and Leyer and Manson [2.31] for open-ended and closed tubes, by Kogarko and Ryzkor [2.31] for closed spherical chambers and by van Wingerden and Zeeuwen.

[2.33] and Tamanini and Chaffee. [2.34] for vented enclosures. For rich propane-air mixtures, van Wingerden and Zeeuwen observed that these instabilities can result in a peak pressure enhancement factor of 8, whereas Tamanini and Chaffee observed enhancement factors of 2 to 9 for stoichiometric methane-air and propane-air mixtures.

Flame acoustic instabilities have usually been associated with relatively slow flames in enclosures that are relatively free of obstacles. Such instabilities have been successfully eliminated by lining the enclosure walls with materials that can absorb acoustic waves. More recently, however, Shepherd and Lee [2.12] reported flame acceleration experiments in tubes with repeated obstacles, with and without an absorbing material on the tube wall. These experiments, performed with a hydrogen-oxygen mixture, indicate that the presence of an absorbing material reduces the final flame velocity from 1000 m/s to 100 m/s. These results would suggest that acoustic flame instabilities may in fact not be limited to slow flames in obstacle-free environments.

The exact nature of the acoustic-flame instabilities have been reviewed by Oran and Gardner [2.35] and have been modelled by Searby and Rochwerger [2.36], Joulin [2.37], Jackson et al. [2.38], and Kansa and Perlee [2.39]. These mechanisms include flame distortion caused by the flame-acoustic wave interaction, and wave amplification caused by the coherence between the acoustic wave and the exothermic energy release (Rayleigh criterion).

Finally, sufficient fast flames can produce a shock wave that can reflect off a wall and interact with the flame. As shown by Markstein and Somers [2.20], this can result in severe flame distortion which can induce flame acceleration and, in extreme cases, cause transition to detonation [2.40, 2.41].

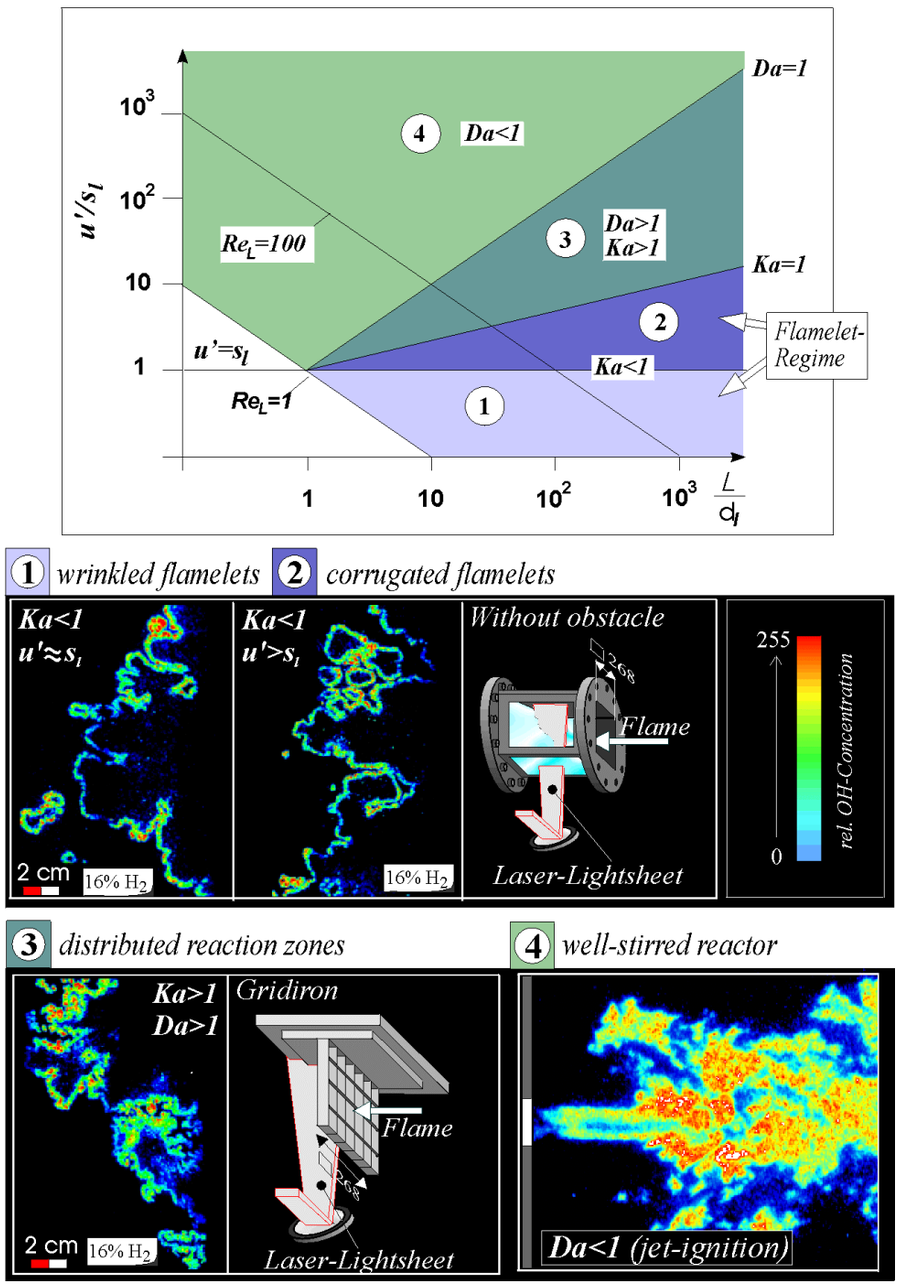

Figure 2.4.2-1 Borghi Diagram (top) categorizing the flame propagation regime in terms of the turbulence intensity, u', the laminar burning velocity, s_l, the integral length scale, L, the laminar flame thickness, d_l, the Damköhler number, Da , the Karlowitz number, Ka, and the turbulent Reynolds number, Re_L. LIPF images (bottom) of flame structure for the various regimes [2.29].

2.4.4 Global and Local Quenching

Flame quenching can occur for a wide spectrum of flame propagation regimes including laminar, wrinkled, and turbulent flames.

2.4.4.1 Quenching of laminar flames and flammability limits

Theoretically, a mixture is flammable, if a flame, regardless of how it was produced, continues propagating within the mixture. However, beyond a certain range of mixture composition, continued propagation of a reaction front is no longer possible because of heat losses to walls and low burned gas temperature. This composition limit is commonly known as the flammability limit. The measured limit can be affected by the size of the apparatus as well as the strength of the ignition source. Coward and Jones [2.42] suggested that tube diameters larger than 5 cm are needed to produce limits that are free of wall effects. They also found that a minimum tube length of 1.2 m is required to avoid the igniter effects. Using a 5-cm-diameter, 1.8-m-long tube, Kumar [2.43] measured the flammability limits for various hydrogen-air-steam mixtures at 100°C and 200°C. These results, summarized in Figure 2.4.4.1-1, show that steam can significantly reduce the range of the flammability. At an initial temperature of 100°C, a mixture is not flammable if it contains more than 63% of steam by volume. Results also show that increasing the gas temperature widens the flammability limits. It was observed that the flammability limits are greatly influenced by the buoyancy effects. The upward propagation limits (assisted by the buoyancy) are different from the downward propagation limits for hydrogen-lean mixtures. Results also show that there is a difference (~5 H_2 vol %) between the upward and the downward flammability limits. However, the difference for the upward and the downward limits is relatively small for hydrogen-rich mixtures. It was also observed that the lean flammability limits are not sensitive to the steam content, whereas the rich flammability limits are greatly affected by the steam content in the mixture. It should be noted that near-flammability-limit mixtures are not very reactive. These mixtures usually cannot support flame acceleration to supersonic velocities and DDT.

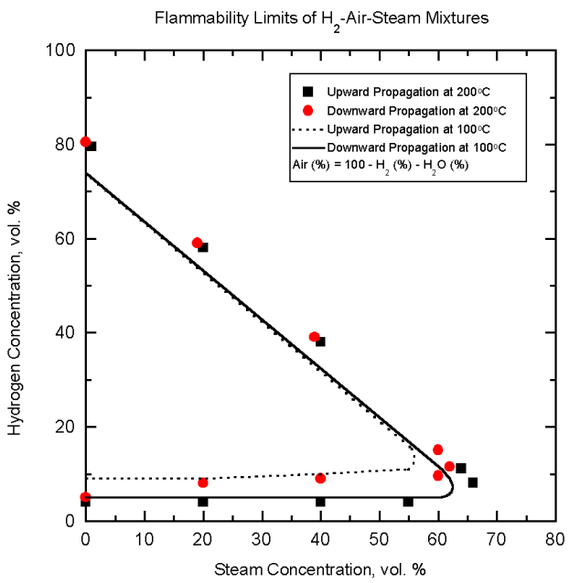

Figure 2.4.4.1-1 Flammability limits for hydrogen-air-steam mixtures [2.43]

2.4.4.2 Quenching of turbulent flames

The same turbulent mixing processes that produce flame acceleration can also result in local or global quenching. For turbulent flames that are in the flamelet regime, this quenching is due to excessive stretching of the laminar flamelets. For more turbulent flames, quenching can occur because of the mixing of cold unburned gas into the distributed reaction zones. The flame-quenching process has been investigated by various authors including Abdel-Gayed and Bradley [2.44], Ballal and Lefebvre [2.45], Checkel and Thomas [2.46], Chomiac [2.47], Phillips [2.48] and Larsen [2.49].

Local quenching is important to the flame acceleration process because it can lead to violent secondary explosions and DDT. Global quenching has been observed for lean flames propagating in tubes filled with obstacles [2.50, 2.51]. It has also been observed when a flame propagates through an orifice into an unconfined area [2.13]. In this case, the minimum quenching diameter increases with the magnitude of the pressure differential generated across the orifice before the arrival of the flame front.

2.4.5 Effects of Buoyancy

Buoyancy affects the early stages of flame propagation and is particularly important for large-scale explosions. These effects are considered to become significant when the Froude number, $Fr = \frac{u^2}{gL}$, is small. There are three potentially important effects of buoyancy. First, the gravitational effect lifts the flame, thereby modifying its path and often bringing it in contact with the top boundary, which can result in local cooling and quenching. Second, for mixtures between the flammability limits for upward and downward propagation, flame propagation may be limited to the top of a channel resulting in incomplete combustion in the bottom section. As can be seen from Figure 2.4.4.1-1, this is more likely to occur for lean hydrogen-air flames where the limits differ significantly for upward and downward propagation. Finally, upward acceleration can result in Rayleigh-Taylor instabilities that can promote acceleration.

2.5 Mechanisms Involved in DDT

2.5.1 Types of DDT Phenomena

Transition from deflagration to detonation can be observed in a wide variety of situations, including flame propagation in smooth tubes or channels [2.52, 2.53], flame acceleration caused by repeated obstacles [2.54-2.56], and jet ignition [2.57-2.60]. The processes leading to detonation can be classified into 2 categories:

1. detonation initiation resulting from shock reflection or shock focusing, and

2. transition to detonation caused by instabilities near the flame front or caused by flame interactions with a shock wave, another flame or a wall, or caused by the explosion of a previously quenched pocket of combustible gas.

The first category essentially involves a direct initiation process where the shock strength is sufficient to auto-ignite the gas and promote detonation. For accidental explosions where the shock is produced by an accelerating flame, this process becomes much more probable when the shock interacts with a

corner or a concave wall that can produce shock focusing. Shock initiation is an important mechanism in maintaining the propagation of quasi-detonations in a channel or a tube filled with obstacles [2.54-2.56]. It has also been found to be very efficient in promoting detonation for relatively slow flames propagating towards an orifice, a corner, or a concave wall [2.61-2.71].

The second category of DDT processes is considerably more complex because it involves a variety of instabilities and mixing processes. Detonation in smooth tubes can occur because of a variety of reasons including (a) DDT ahead of the turbulent flame brush, (b) DDT inside the flame brush, or (c) DDT resulting from the interaction between the flame front with a reflected shock wave. DDT can also occur in a flame jet because of a flame-vortex interaction that promotes a suitable temperature and concentration gradient for inducing DDT by means of the SWACER mechanism discussed in Section 2.5.2.

2.5.2 Underlying Mechanisms

Although DDT appears though a variety of seemingly unrelated phenomena, there is increasing evidence that these phenomena may be controlled by a single underlying mechanism. It has been suggested by Zel'dovich et al. [2.72-2.74] and Lee et al. [2.75] that induction time gradients associated with temperature and concentration gradients may be ultimately responsible for a wide range of detonation initiation observations. The mechanism proposed by these authors rests on the formation of an induction time gradient that can produce a spatial time sequence of energy release. This sequence can then produce a compression wave that is gradually amplified into a strong shock wave that can auto-ignite the mixture and produce DDT. This process of shock wave amplification by coherent energy release (SWACER) was used by Lee et al. [2.75] and Yoshikawa [2.76] to explain the shockless photo-initiation of gaseous detonations.

Numerous calculations have been presented in the literature to demonstrate the SWACER or Zel'dovich gradient process. These include the early studies by Zel'dovich et al. [2.72-2.74], Lee et al. [2.75], Yoshikawa [2.76] and those by Yoshikawa, Thibault and Hassam that were discussed in the review papers by Lee and Moen [2.77] and Shepherd and Lee [2.12]. More recent calculations have been performed by Clark [2.78], Frolov et al. [2.79], Dorofeev et al. [2.80-2.82], Gelfand et al. [2.83], Smijanovski and Klein [2.84], Khokhlov et al. [2.85, 2.86], and others [2.87-2.97]. These authors have established a strong theoretical foundation for the amplification process, and have demonstrated the role of the SWACER or Zel'dovich gradient mechanism for various DDT and direct initiation problems. One observation from these studies is that the minimum size of the pre-established gradient required for DDT is approximately 10 times the detonation cell size (see Section 3.2.3). There is also an optimal range of induction time gradients that can promote a shock amplification process that can lead to DDT [2.85, 2.96].

Because temperature and concentration gradients are formed by a wide variety of processes, the SWACER mechanism is believed to be an underlying mechanism for a wide variety of detonation phenomena including

1. direct detonation initiation that is due to the temperature gradient behind the leading shock,

2. detonation initiation that is due to shock focusing,

3. DDT in tubes that is caused by the temperature gradient in the boundary layer or between a fast flame and the leading shock,

4. DDT that is due to pre-compression at the end of a channel by a slow flame,

5. DDT in rough or obstacle-filled tubes,

6. jet initiation caused by temperature and concentration gradients in the flame/vortex structure, and

7. DDT in multi-phase systems resulting from the temperature relaxation caused by the particles.

In spite of the number of SWACER calculations that can be found in the literature, few of these can be directly and convincingly linked to a particular experimental result. This is particularly true for problems involving turbulent mixing for which calculations usually assume a spontaneous formation of a temperature or concentration gradient or both. The actual formation of such gradients involves a variety of turbulent mixing and combustion mechanisms. These mechanisms introduce additional instabilities that must be addressed by the calculations in order to be truly predictive. Such difficulties have recently been addressed by Khokhlov et al. [2.85, 2.86], who investigated the very difficult problem of DDT caused by shock-flame interaction. This type of DDT, which has been observed by Thomas et al. [2.41], involves a Meshov-Richmeyer instability, where the reflected shock interacts with the flame front. The severe flame distortion produced by this instability then produces Kelvin-Helmholtz instabilities, which increase the flame area and the rate of combustion. The very high resolution calculations of Khokhlov et al. [2.85, 2.86] have been able to resolve these instabilities and capture the DDT process that occurs inside a temperature gradient. These Navier-Stokes calculations remain limited in that they do not directly account for the fine-scale turbulent mixing. Nevertheless, they represent one of the most successful efforts so far to isolate the SWACER mechanism for a particular experimental DDT observation.

2.6 Recent Experimental Results

The above description of FA and DDT mechanisms has included recent experimental data obtained from various laboratories in Europe and in North America:

1. The large-scale deflagration experiments performed in the RUT facility [2.98]: These experiments, along with previous DDT experiments, contributed to the formulation of the 7λ criterion (Figure 2.6-1).

2. The experiments performed by Thomas et al. [2.41, 2.99] for DDT produced by the interaction of a reflected shock with a flame kernel: These experiments, along with the calculations of Khokhlov et al. [2.85, 2.86] have shed considerable light on the DDT phenomenon and the underlying SWACER mechanism (Figure 2.6-2).

3. The shock focusing experiments performed by Chan et al. [2.100] and Gelfand and Khomik. [2.101]: These experiments have demonstrated that a relatively weak shock can trigger DDT when concave reflecting surfaces are present in the enclosure (Figure 2.6-3),

4. The detailed LIPF experiments performed by the Technical University of Munich on flame propagation and jet ignition [2.103]. (Figure 2.6-4).

5. Experiments on DDT induced by a focused shock wave were performed in FZK for various focusing geometry: Three test series addressing three different DDT modes in a combustion tube (12 m long, 35 cm ID) were performed [2.102]. Detailed results from these experiments are presented in Appendix E.

6. Experiments were performed at BNL [2.110] in the High-Temperature Combustion Facility (HTCF) to study flame acceleration and DDT with and without venting at high initial temperatures (up to 650 K) (Figures 2.6-5 and 2.6-6). In these experiments, orifices with a blockage ratio of 0.43 (spaced 1 tube diameter apart) were used to induce and to promote flame acceleration. The central element of the HTCF is a 27-cm-inner-diameter and 21.3-m-long cylindrical test vessel designed for a maximum allowable working pressure of 10.0 MPa at 700 K.

2.7 Pressure Development and Structural Response

2.7.1 Pressures Associated with Flames, Detonations, and DDT

Flame acceleration in an enclosure produces pressures that, in some cases, may be high enough to threaten the survival of the enclosure or its substructures. The pressure developed inside the enclosure depends on

1. the size of the combustible gas region,

2. the concentration of the combustible gas, and

3. the size of the enclosure and the arrangement of the obstacles.

In the case of a uniform mixture inside the enclosure, and no heat losses, the peak pressure achieved in the enclosure can vary between the constant volume combustion pressure to the very high pressures associated with DDT. As indicated by Craven and Greig [2.104], the pressure produced by DDT depends on the flame propagation process prior to DDT. The worst-case scenario proposed by Craven and Greig involves the transition to detonation on a reflected shock produced by a fast flame. Calculations indicate that the peak pressure produced on the wall of an enclosure by such an event can be an order of magnitude higher than the detonation pressure for the mixture. The Craven and Greig scenario has been observed in the laboratory by Kogarko [2.105], Chan et al. [2.100] and Zhang et al. [2.106]. In the latter study, a peak reflected pressure of 250 atm was observed for a hydrocarbon-air mixture at an initial pressure of 1 atm.

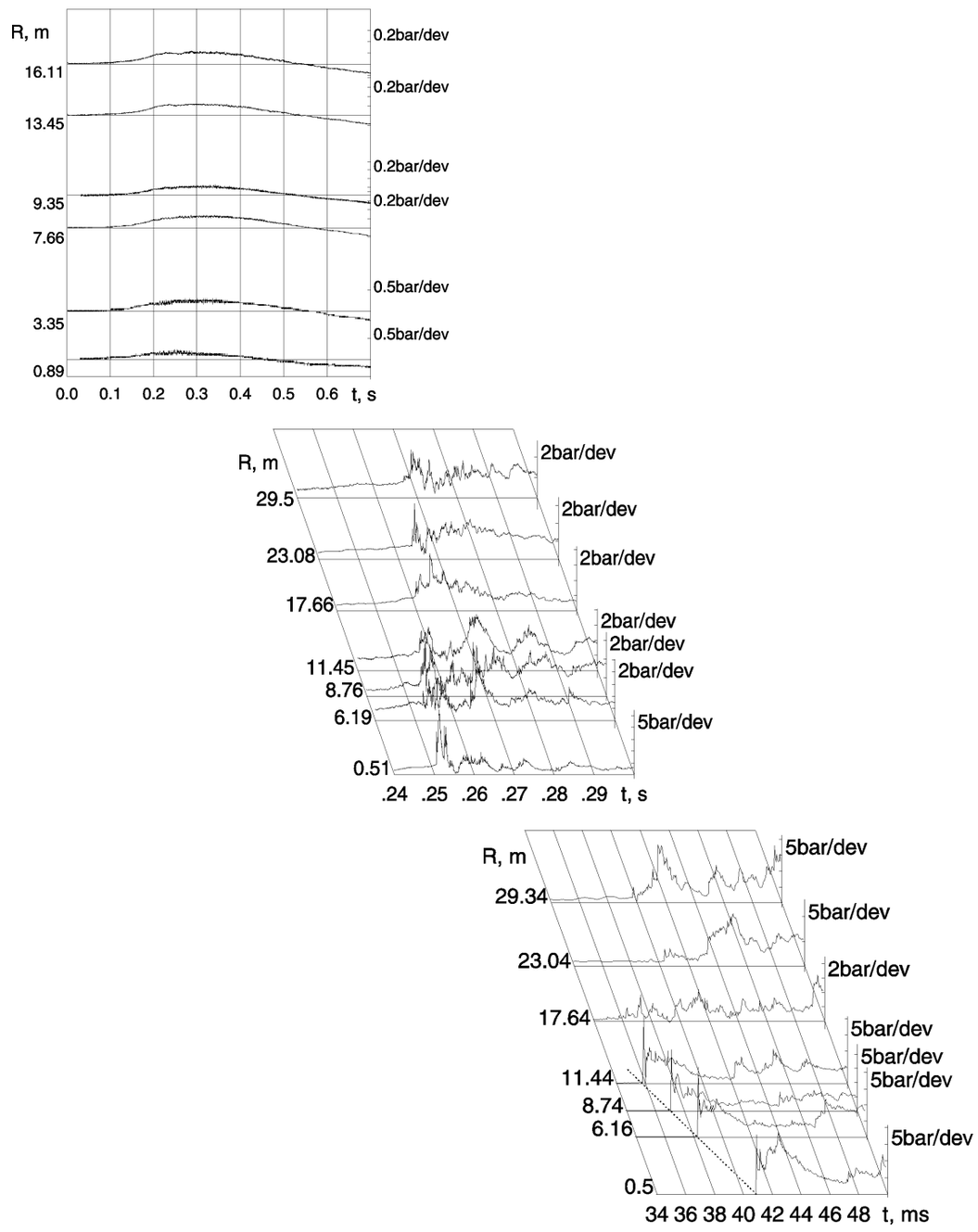

Figure 2.6-1 Pressure histories obtained in RUT Facility. Top: Slow deflagration, 8% H_2 in air. Middle: Fast turbulent deflagration, 19% H_2 in air. Bottom: DDT, 42% H_2 in air. Concentrations correspond to average values within the 310 m^3 vented enclosure.

It should be noted that the peak pressure alone is insufficient to determine the vulnerability of a structure. Pressure records associated with DDT or a stable detonation display a sharp pressure rise followed by a decay, which is relatively rapid for DDT. Slow and fast deflagrations, on the other hand, display a more gradual pressure rise and decay. The details of the pressure histories can be very important in assessing the response of a particular structure.

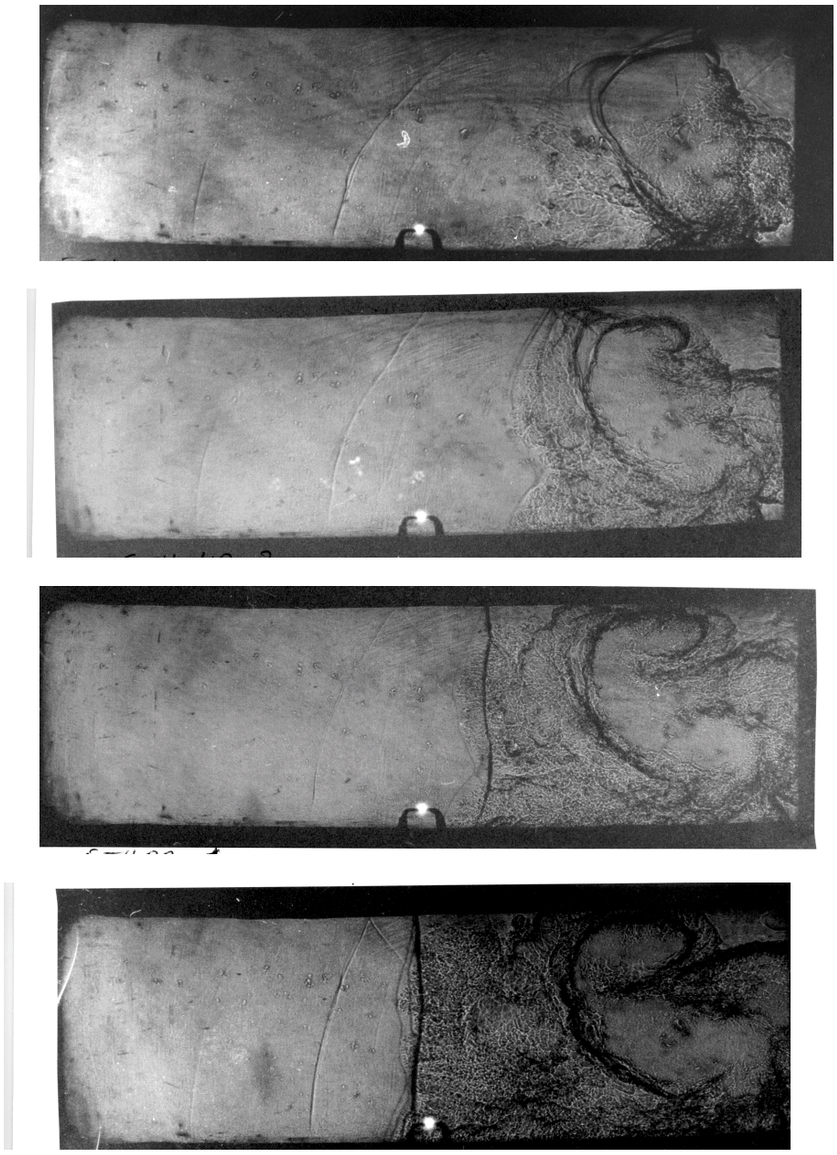

Figure 2.6-2 Schlieren images of DDT resulting from flame-shock interaction [2.99]

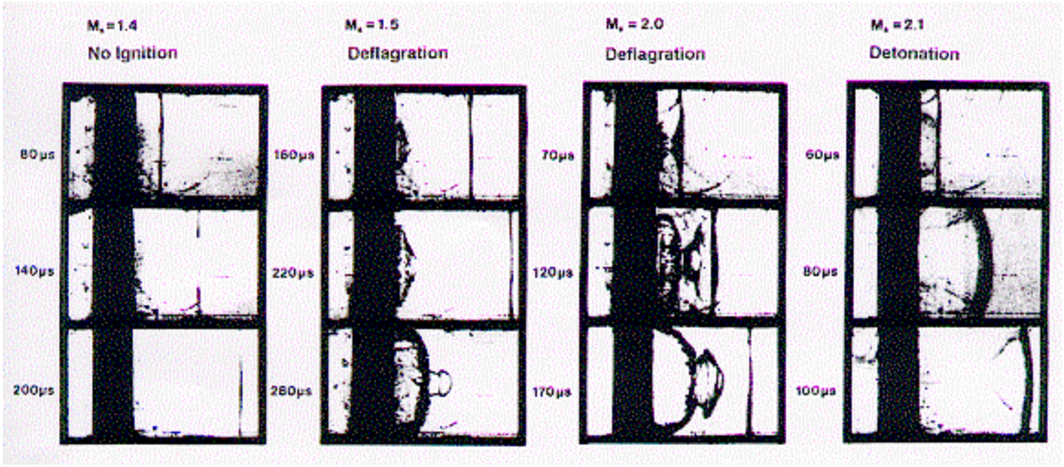

Figure 2.6-3 Schlieren photographs showing the outcomes resulting from a collision of a shock wave with a hemispherical cup (dia.= 3 cm) . (Chan et al. [2.100])

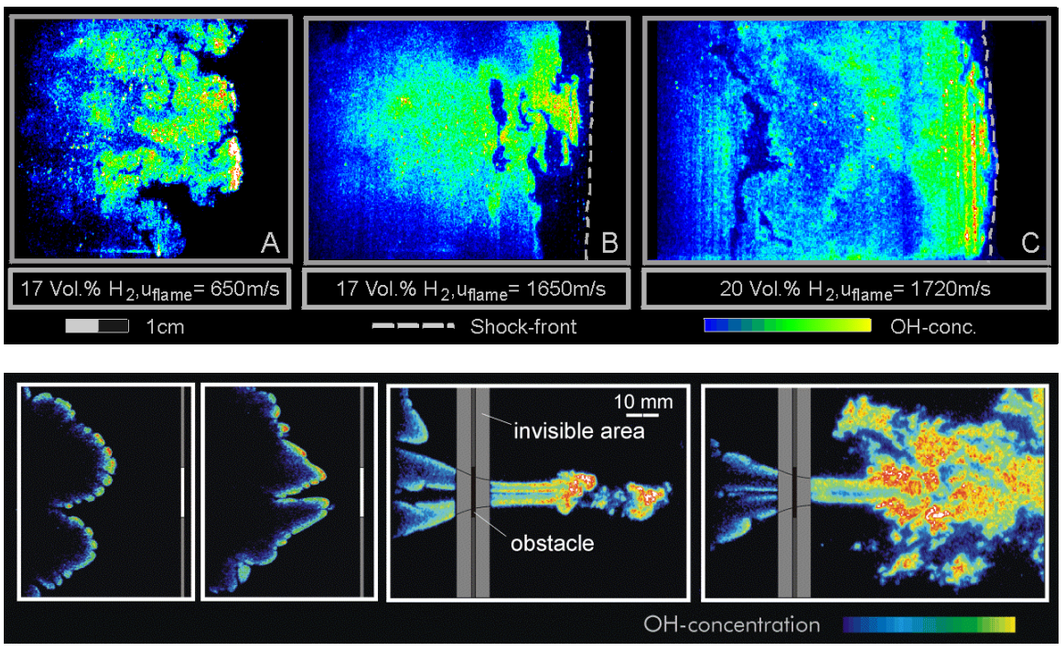

Figure 2.6-4 LIPF images from the Technical University of Munich. Top images of a fast propagating flame, a detonation for a mixture close to the detonation limit for the facility, and a fully developed detonation [2.26]. Bottom: Flame-jet ignition for a 12% hydrogen-air flame [2.27]. The combustion-regime behind the free jet of a direct ignition can be assigned to the well-stirred reactor regime in the Borghi diagram.

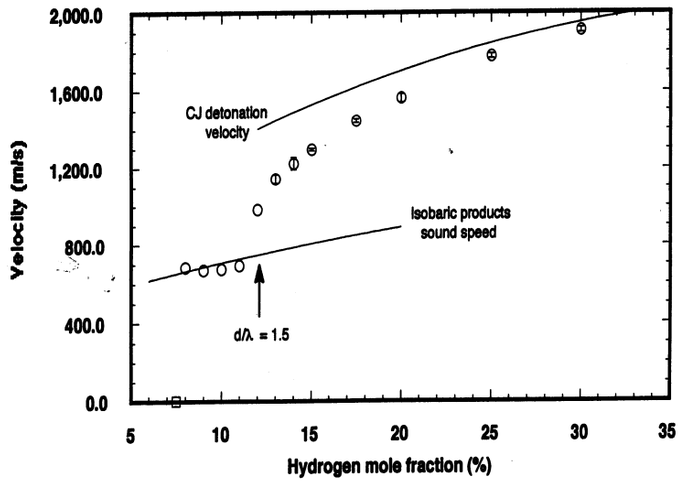

Figure 2.6-5 Combustion front velocity versus hydrogen mole fraction for hydrogen-air mixtures at 500 K and 0.1 MPa at the HTCF at BNL. Open circles denote the average velocity over roughly the second half of the vessel, and error bars represent the standard deviation in the measured velocity. Open squares denote the maximum flame velocity for slow deflagration.

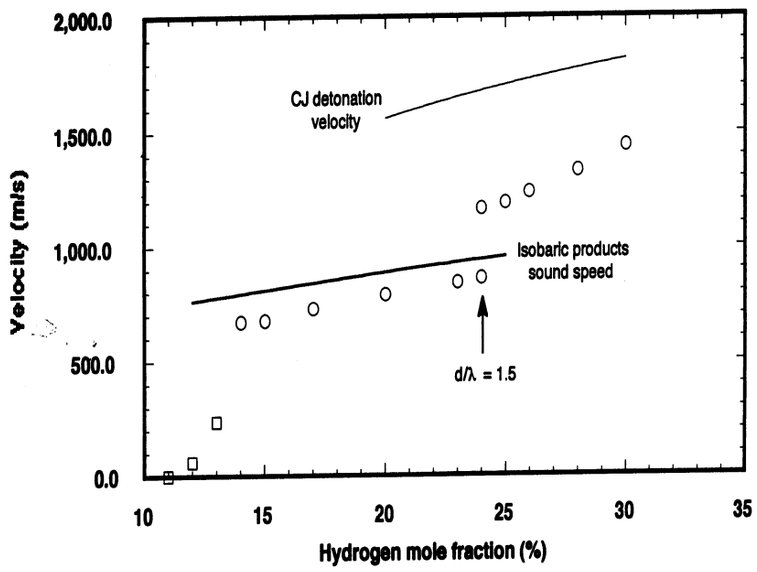

Figure 2.6-6 Combustion front velocity versus hydrogen mole fraction for hydrogen-air mixtures with 25% steam at 500 K and 0.1 MPa at the HTCF at BNL. Open circles denote the average velocity over roughly the second half of the vessel, and error bars represent the standard deviation in the measured velocity. Open squares denote the maximum flame velocity for slow deflagration.

2.7.2 Structural Response

Important factors affecting the response of a structure to a transient pressure loading include the peak pressure and the length of the rise and decay times compared to the characteristic response time of the structure.

Table 2.7.2-1 lists typical natural frequencies for various nuclear reactor components based on the work of Breitung et al. [2.107], and Breitung and Redlinger [2.108] and Studer and Petit [2.109]. Concrete containment building frequencies were obtained by Studer and Petit based on an eigen-frequency analysis for a typical PWR reactor. It can be seen that the frequency range that is of interest for nuclear reactors is approximately 5 to 500 Hz.

Breitung and Redlinger [2.108] performed a detailed 1-degree-of-freedom analysis for a set of representative time histories for scenarios involving slow flames, fast flames, stable detonations, and DDT. Figure 2.7.2-1 displays the frequency dependence of the effective static pressure ratio, P_{eff}, that would produce the same deflection as the transient loading. The frequency range in this figure corresponds to the range of natural frequencies for nuclear reactor components shown in Table 2.7.2-1. It can be seen from this figure that the stable detonation is the most severe combustion mode throughout this frequency range. In the range of 5 to 25 Hz, which is characteristic of the frequency response of concrete nuclear reactor containment buildings, the stable detonation and fast deflagrations display a similar response, whereas DDT and slow deflagrations exhibit a weaker response. This finding differs from that reported by Studer and Petit (Table 2.7.2-2), who observe significantly larger displacements for fast deflagrations with progressively lower responses for DDT and a stable detonation. These authors concluded that the fast deflagration is the most severe scenario for a concrete containment building. The different conclusions emerging from these 2 studies could be attributed to the different structural response models or to the different pressure histories used to characterize the various flame and detonation regimes. Assessment of the vulnerability of nuclear containment buildings and substructures will require more work in the analysis of experimental results and in the development of detailed models.

Table 2.7.2-1 Typical natural frequencies for various nuclear reactor components

Structure Type	Frequency (Hz)
Spherical Steel Containment (Bending Mode) [2.108]	6-12
Spherical Steel Containment (Membrane Mode) [2.108]	50
Concrete Containment [2.108]	5-8
Concrete Containment [2.109]	12-22
Stiff Reinforced Concrete Substructures [2.108]	<500
Technical Installations [2.108]	100-400

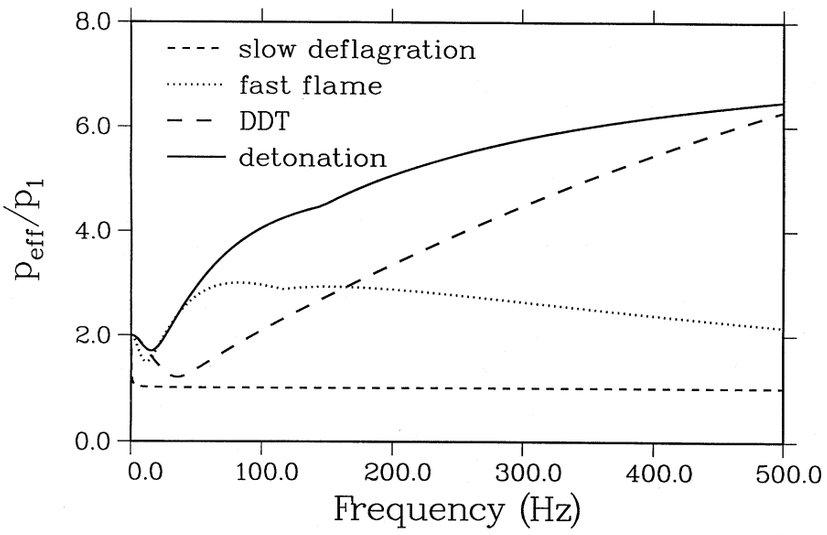

Figure 2.7.2-1 Normalized effective static pressure for a frequency range relevant to nuclear reactor applications [2.108]. Pressures are normalized relative to the long-term combustion pressure

Table 2.7.2-2. Containment wall displacements for the various combustion models and structural eigen frequencies [2.109]

Eigen Frequency (Hz)	Fast Deflagration (mm)	DDT (mm)	Stable Detonation (mm)
12.47	45	10	7.4
14.01	32	9.9	7.3
18.73	22	9.4	7.0
22.01	16	9.0	6.7

2.8 Summary

Flame acceleration and transition to detonation are complex phenomena. Within the scope of this chapter, it is impossible to review and discuss all the studies in the subject area. As a result, only some key studies relevant to the nuclear industry have been included. Nevertheless, the material presented in this chapter represents a snapshot of current understanding of the phenomena.

In Section 2.2, the regimes of various eventual outcomes of flame acceleration are discussed. These possible outcomes are well understood; they depend on the initial gas mixture composition and the boundary conditions such as walls and obstruction configurations. However, the rate at which these outcomes are reached is not well understood. As indicated in Section 2.3, the degree of confinement

of the gas mixture dominates the flame acceleration rate. It is not possible to estimate the flame acceleration rate for a given set of conditions. More work in this area is definitely needed to determine the effects of confinement on flame acceleration.

Sections 2.4 and 2.5 describe the mechanisms responsible for flame acceleration and transition to detonation. Qualitatively, these mechanisms are also well understood. However, the current understanding of the phenomena still cannot enable analysts to develop models that can predict flame acceleration and eventual transition to detonation (to be discussed in Chapter 4). Nevertheless, new findings have helped these analysts to refine their models and provide direction for future works.

Section 2.6 outlines some of the recent works in the area of FA and DDT. This work includes large-scale experiments in the RUT facility and detailed flame structure measurement using LIPF and schlieren photography. Only a brief discussion is given here. Readers should go to the cited references to get the details of these works. Section 2.7 discusses briefly the response of various structures subjected to a pressure load of an accelerated flame or a detonation wave. As mentioned in this section, the knowledge in this area is still at its infant state. More work is definitely needed in this area in order to estimate the structural response in any acceptable certainly.

Although FA and DDT are qualitatively understood, they remain a big challenge to scientists to develop models capable of predicting the dynamic process and the eventual consequence of these phenomena.

2.9 References

2.1 H.Gg Wagner, *Some Experiments about Flame Acceleration, Fuel-Air Explosions*, University of Waterloo Press, 1982, 77-99.

2.2 I.O. Moen, M. Donato, R. Knystautas and J.H.S. Lee, Flame Acceleration Due to Turbulence Produced by Obstacles, Combustion ands Flame, Vol. 39, 1980, 21-32.

2.3 J.H.S. Lee, R. Knystautas and C.K. Chan, Turbulent Flame Propagation in Obstacle-Filled Tubes, In 20th Symposium (International) on Combustion, The Combustion Institute, 1985, 1663-1672.

2.4 C.K. Chan, J.H.S. Lee, I.O. Moen and P. Thibault, Turbulent Flame Acceleration and Pressure Development in Tubes, In Proc. of the First Specialist Meeting (International) of the Combustion Institute, Bordeaux, France, 1981, 479-484.

2.5 B.H. Hjertager, K. Fuhre, S.J. Parker and J.R. Bakke, Flame Acceleration of Propane-Air in Large-Scale Obstacled Tube, Progress in Astronautics and Aeronautics, Vol. 94, AIAA, 1983, 504-522.

2.6 I.O. Moen, J.H.S. Lee, G.H. Hjertager, K. Fuhre and R.K. Eckhoff, Pressure Development due to Turbulent Flame Acceleration in Large-Scale Methane-Air Explosions, Combustion and Flame, Vol. 47, 1982, 31-52.

2.7 C.J.M. Van Wingerden and J.P. Zeeuwen, Investigation of the Explosion-Enhancing Properties of a Pipe-Rack-Like Obstacle Array, Progress in Astronautics and Aeronautics Vol.106, 1986, 53.

2.8 J.C. Cummings, J.R. Torczynski and W.B. Benedick, Flame Acceleration in Mixtures of Hydrogen and Air, Sandia National Laboratory Report, SAND-86-O173, 1987.

2.9 S.B. Dorofeev, private communication, 1999.

2.10 K.I. Shchelkin, Effect of Tube Surface Roughness on Origin and Propagation of Detonation in Gas, Journal of Experimental and Theoretical Physics (USSR), 10, 1940, 823-827.

2.11 H. Guenoche, and N. Manson, Influence des Conditions aux Limites sur la Propagation des Ondes de Choc et de Combustion, Rev. de l'Inst. Francais de Petrole, No. 2, 1949, 53-69.

2.12 J.E. Shepherd and J.H.S. Lee, On the Transition from Deflagration to Detonation, *Major Research Topics in Combustion*, Editors: M.Y. Hussaini, A. Kumar, R.G. Voit, Springer Verlag, Berlin, 1991.

2.13 P. Thibault, Y.K. Liu, C.K. Chan, J.H. Lee, R. Knystautas, C. Guirao, B. Hjertager and K. Fuhre, Transmission of an Explosion Through an Orifice. Proc. of the 19th Symposium (International) on Combustion, Haifa, Israel, 1982, 599-606.

2.14 C.K. Chan, I.O. Moen and J.H.S. Lee, Influence of Confinement on Flame Acceleration Due to Repeated Obstacles, Combustion and Flame 49, 1983, 27-39.

2.15 R.K. Kumar W.A. Dewit and D.R. Greig, Vented Explosion of Hydrogen/Air Mixtures in a Large Volume, Combustion Science and Technology 66, 1989, 251-266.

2.16 H. Pfortner, H. Schneider, W. Drenkhahn and C. Koch, Flame Acceleration and Build-Up in Partially Confined Clouds, Presented at the 9th International Colloquium on Dynamics of Explosions and Reactive Systems, Poitiers, France, 1983.

2.17 M.P. Sherman, S.R. Tieszen and W.B. Benedick, FLAME Facility: The Effect of Obstacles and Transverse Venting on Flame Acceleration and Transition to Detonation for Hydrogen/Air Mixtures at Large Scale, Sandia National Laboratories Report, NUREG/CR-5275 or SAND-85-1264, 1989.

2.18 G. Ciccarelli, T. Ginsberg, J. Boccio, C. Economos, K. Sato and M. Kinoshita, Detonation Cell Size Measurements and Predictions in Hydrogen-Air-Steam Mixtures at Elevated Temperatures, Combustion and Flame, Vol. 99. No. 2, 1994, 212-220.

2.19 M. Kaneshige, and J.E. Shepherd, Detonation Database, Report FM-97-8, GALCIT, Explosion Dynamics Laboratory, 1997.

2.20 G.H. Markstein and L.M. Somers, Cellular Flame Structure and Vibratory Flame Movement in N-Butane-Methane Mixtures, Fourth Symposium (International) on Combustion, Williams & Wilkins, 1964.

2.21 G.H. Markstein, *Nonsteady Flame Propagation*, Pargamon Press, Oxford, England, 1964.

2.22 P. Clavin and F.A. Williams, Effects of Molecular Diffusion and Thermal Expansion on the Structure and Dynamics of Premixed Flames in Turbulent Flows of Large Scale and Low Intensity, Journal of Fluid Mechanics, Vol. 116, 1981, 252-282.

2.23 G. Joulin and P. Clavin, Linear Stability Analysis of Nonadiabatic Flames: Diffusion Thermal Model, Combustion and Flame, Vol. 35, 1979, 139-153.

2.24 P. Pecle and P. Clavin, Influence of Hydrodynamics and Diffusion Upon the Stability of Laminar Premixed Flames, Journal of Fluid Mechanics, Vol. 124, 1982, 219-237.

2.25 M. Kuzenetsov, V. Alekseev, A. Bezmelnitsyn, W. Breitung, S. Dorofeev, I. Matsukov, A. Veser and Yu. Yankin, Effect of Obstacle Geometry on Behavior of Turbulent Flames, IAE-6137/3 FZKA-6328, 1999.

2.26 N. Ardey, Structure and Acceleration of Turbulent Hydrogen-Air-Flames Within Obstructed Confinements, PhD Thesis, Technical University of Munich, 1998.

2.27 M. Jordan, Ignition and Combustion of Premixed Turbulent Jets, PhD Thesis, Technical University of Munich, 1999.

2.28 T. Hirano, Behaviour of Propagating Premixed Flames, Hikita Memorial Lecture.

2.29 N. Peters, Laminar Flamelet Concepts in Turbulent Combustion, 21st Symposium (International) on Combustion, The Combustion Institute, Pittsburgh, 1986, 1231-1256.

2.30 H. Guenoche, Rev. Inst. Franc. Petrole, Vol. 4, 1949, 48.

2.31 J.C. Leyer and N. Manson, Development of Vibratory Flame Propagation in Short Closed Tubes and Vessels Thirteenth Symposium (International) on Combustion, The Combustion Institute, Pittsburgh, 1971, 551-557.

2.32 S.M. Kogarko, and D.L. Ryzhkov, Journal of Technology and Physics USSR, Vol. 31, 1961, 211.

2.33 C.J.M. Van Wingerden and J.P. Zeeuwen, On the Role of Acoustically Driven Flame Instabilities in Vented Gas Explosions and Elimination, Combustion and Flame, Vol. 51, 1983, 109-111.

2.34 F. Tamanini and J.L. Chaffee, Turbulent Vented Gas Explosions with and Without Acoustic Waves, Symposium (International) on Combustion, The Combustion Institute, Pittsburgh, 1992, 1845-1851.

2.35 E.S. Oran and J.H. Gardner, Chemical-Acoustic Interactions in Combustion Systems, Progress in Energy and Combustion Science, Vol. 11, 1985, 253-276.

2.36 G. Searby and D. Rochwerger, A Parametric Acoustic Instability in Flames, Journal of Fluid Mechanics, Vol. 231, 1991, 529-543.

2.37 G. Joulin, On the Response of Premixed Flames to Time Dependent Stretch and Curvature, Combustion Science and Technology, Vol. 97, 1994, 219.

2.38 T.L. Jackson, M.G. Macaraeg and M.Y. Hussaini, The Role of Acoustics in Flame/Vortex Interactions, Journal of Fluid Mechanics, Vol. 254, 1993, 259-603.

2.39 E. Kansa and H.E. Perlee, Constant-Volume Flame Propagation: Finite-Sound-Speed Theory, United States Department of the Interior, Bureau of Mines, Report of Investigations 8163, 1976.

2.40 T. Scarincini, J.H. Lee, G.O. Thomas, R. Brambrey and D.H. Edwards, Progress in Astronautics and Aeronautics, AIAA, Vol. 152, 1993, 3-24.

2.41 G.O. Thomas, C.J. Sands, R.J. Brambrey and S.A. Jones, Experimental Observations of the Onset of Turbulent Combustion Following Shock-Flame Interaction, Proceedings of the 16th International Colloquium on the Dynamics of Explosions and Reactive Systems, Cracow, 1997, 2-5.

2.42 H.F. Coward and G.W. Jones, Limits of Flammability of Gases and Vapors, U.S. Bureau of Mines Bulletin 503, 1953.

2.43 R.K. Kumar, Flammability Limits of Hydrogen-Oxygen-Diluent Systems: Horizontal Propagation Limits, AECL Report, WNRE-626, 1985.

2.44 R.G. Abdel-Gayed and D. Bradley, The Influence of Turbulence upon the Rate of Turbulent Burning, Proc. of the First Specialist Meeting on Fuel-Air Explosions, Montreal, Canada, 1981.

2.45 D.R. Ballal and A.H. Lefebvre, The Influence of Flow Parameters on Minimum Ignition Energy and Quenching Distance, 15th Symposium (International) on Combustion, The Combustion Institute, Pittsburgh, 1975, 1473.

2.46 M.D. Checkel and A. Thomas, Turbulent Combustion of Premixed Flames in Closed Vessels, Combustion and Flame, Vol. 96, 1994, 351-370.

2.47 J. Chomiac, Flame Development from an Ignition Kernel in Laminar and Turbulent Homogeneous Mixtures, 17th Symposium (International) on Combustion. The Combustion Institute, Pittsburgh, 1979, 25.

2.48 H. Phillips, The Save Gap Rivisited, Progress in Astronautics and Aeronautics, AIAA, Vol. 114, 1988, 77-96.

2.49 O. Larsen, A Study of Critical Dimensions of Holes for Transmission of Gas Explosions and Development and Testing of a Schlieren System for Studying Jets of Hot Combustion Products, Thesis for the degree of Cand. Scient., University of Bergen, Norway, 1998.

2.50 J.H. Lee, R. Knystautas and C.K. Chan, Turbulent Flame Propagation in Obstacle-Filled Tubes, 20th Symposium International) on Combustion, The Combustion Institute, 1985, 1663-1672.

2.51 R. Knystautas, J.H.S. Lee, O. Peraldi, and C.K. Chan, Transmission of a Flame from a Rough to a Smooth Wall Tube, Progress in Astronautics and Aeronautics, Vol. 106, 1986, 37-52.

2.52 B. Lewis and G. von Elbe, *Combustion Flames and Explosions of Gases*, 2nd Edition Academic Press, New York, 1961.

2.53 P.A. Urtiew and A.K. Oppenheim, Experimental Observations of Transition to Detonation in an Explosive Gas, Proc. of the Royal Society, Vol. A295, 1966, 13-28.

2.54 O. Peraldi, R. Knystautas and J.H. Lee, Criteria for Transition to Detonation in Tubes, 21st Symposium (International) on Combustion, The Combustion Institute, 1988, 1629.

2.55 C.K. Chan and D.R. Greig, The Structures of Fast Deflagrations and Quasi-Detonations", 22nd Symposium (International) on Combustion, The Combustion Institute, 1988, 1733-1739.

2.56 A. Teodorczyk, J.H.S. Lee and R. Knystautas, Propagation Mechanisms of Quasi-Detonations, 22nd Symposium (International) on Combustion, The Combustion Institute, 1988, 1723-1731.

2.57 F. Carnasciali, J.H. Lee, R. Knytautas and F. Fineschi, Turbulent Jet Initiation of Detonation", Combustion and Flame, Vol. 84, 1991, 170.

2.58 D.J. MacKay, S.B. Murray, I.O. Moen and P.A. Thibault, Flame-Jet Ignition of Large Fuel-Air Clouds, 22nd Symposium (International) on Combustion, The Combustion Institute, 1988, 1339-1353.

2.59 R. Knystautas, J.H. Lee, I. Moen and H.G. Wagner, Direct Initiation of Spherical Detonation by a Hot Turbulent Gas Jet, 17th Symposium (International) on Combustion, The Combustion Institute, Pittsburgh, 1979, 1235-1245.

2.60 M. Schildnecht, W. Geiger and M. Stock, Progress in Astronautics and Aeronautics, Vol. 94, 1985, 474-490.

2.61 A.A. Borisov, B.E. Gelfand, G.I. Skachkov et al., Selfignition of Gaseous Mixtures by Focusing of Reflected Shock Waves, Chimicheskaya Phisika, Vol. 7, No. 12, 1988, 1387.

2.62 A. Borisov, B. Gelfand, G. Skatchkov, et al., Ignition of Gaseous Combustible Mixtures in Focused Shock Waves, Current Topics in Shock Waves, Proc. of the 17th ISSW, AIP, N.Y., 1990, 696-701.

2.63 C.K. Chan, D. Lau, P.A. Thibault and J.D. Penrose, Ignition and Detonation Initiation by Shock Focussing, 17th International Symposium on Shock Waves and Shock Tubes, Lehigh University, Bethlehem, Pennsylvania, USA, July 17-21, 1989, AIP Proceedings 208, 1990, 161-166.

2.64 C.K. Chan, Initiation of Detonation Induced by a Focused Shock Wave, 15th International Colloquium on Explosion and Reactive Systems, 1994.

2.65 B.E. Gelfand, S.M. Frolov, S.P. Medvedev and S.A. Tsyganov, Three Cases of Shock Wave Focusing in a Two Phase Combustible Medium, Shock Waves, Proceedings, Sendai, Japan, 1991, Springer Verlag, Vol II, 1992, 837-842.

2.66 C.K. Chan, A. Guerrero and D. McCooeye, Shock Induced Transition to Detonation, Paper at 2nd Canadian and German Workshop, 1993.

2.67 O.V. Achasov, A.A. Labuda, O.G. Penzijakov and R.M. Pushkin, Shock Waves Initiation of Detonation in Semiclosed Cavity, Chimicheskaya Phisika, Vol. 12, No. 5, 1993, 714-716.

2.68 M. Rose, P. Roth and U. Uphoff, Ignition of Reactive Gas by Focusing of Shock Wave, Proc. of 16th ICDERS, Krakow, 1997, 554-556.

2.69 V.Yu. Gidaspov, I.A. Ivanov and I.A.,Krinlov, Numerical Modeling of Detonation in Focusing Channel, Mathem. Modeling, Vol. 4, No. 4, 1992, 85-88.

2.70 Detonation Ignition Characteristics of H_2-Air Mixtures Under Conditions of Shock Focusing, IChPh RAS @ INR FZK Research Report, 1993.

2.71 Complete Experimental Investigation of Shock Wave Focusing Phenomena in H_2 + Air Mixtures with Additives", IChPh RAS @ INR FZK Research Report, 1994.

2.72 Ya. B. Zel'dovich, V.B. Librovich, G.M. Makhviladze and G.I. Sivashinsky, On the Development of Detonation in a Non-Uniformly Preheated Gas, Astronautica Acta, Vol. 15, 1970, 313-321.

2.73 Ya. B. Zel'dovich, Regime Classification of an Exothermic Reaction with Non-Uniform Initial Conditions, Combustion and Flame, Vol. 39, 1990, 211-214.

2.74 Ya. B. Zel'dovich, B.E. Gelfand, S.A. Tsyganov, S.M. Frolov and A.N. Polenov, Concentration and Temperature Non-Uniformities (CTN) of Combustible Mixtures as a Reason of Pressure Generation, 11th Colloquium on Dynamics of Explosions and Reactive Systems (ICDERS), Warsaw, Vol. 89, 1988.

2.75 J.H.S. Lee, R. Knystautas and N. Yoshikawa, Photochemical Initiation and Gaseous Detonations, Acta Astronautica, Vol. 5, 1978, 971-972.

2.76 N. Yoshikawa, Coherent Shock Wave Amplification in Photo-Chemical Initiation of Gaseous Detonations, PhD Thesis, Department of Mechanical Engineering, McGill University, Montreal, Quebec, Canada, 1980.

2.77 J.H.S. Lee and I.O. Moen, The Mechanisms of Transition from Deflagration to Detonation in Vapor Cloud Explosions, Progress in Energy and Combustion Science, Vol. 6, 1980, 359-389.

2.78 J.F. Clark, Fast Flames, Waves and Detonations, Progress in Energy and Combustion Science, Vol. 15, 1989, 241-271.

2.79 S.M. Frolov, B.E. Gelfand and S.A. Tsygonov, Spontaneous Combustion Regimes, Soviet Journal of Explosion and Combustion Shock Waves, Vol. 28, No. 5, 1992, 132-27.

2.80 S.B. Dorofeev, A.A. Efimenko and A.S. Kochurko, Numerical Study of Detonation Self-Initiation Conditions, 15th ICDERS, Boulder, Colorado, 1995, 425-428.

2.81 S.B. Dorofeev, A.V. Bezmelnitsin and V.P. Sidorov, Transition to Detonation in Vented Hydrogen-Air Explosion, Combustion and Flame, Vol. 103(3), 1995, 243-246.

2.82 S.B. Dorofeev, A.S. Kochurko, A.A. Efimenko and B.B. Chaivanov, Evaluation of Hydrogen Explosion Hazard, Nuclear Engineering and Design, Vol. 148, No. 2, 1994, 305-310.

2.83 B.E. Gelfand, S.P., Medvedev, A.N. Polenov, S.V. Khomik and A.M. Bartenev, Basic Selfignition Regimes and Conditions for their Realization in Combustible Gas Mixtures, Combustion, Explosion and Shock Waves, Vol. 33, No. 2, 1997, 127-133.

2.84 V. Smijanovski and R. Klein, Flame Front Tracking via In-Cell Reconstruction, Proceedings of the 5th International Conference on Hyperbolic Systems, SUNY, Stony Brook, June 1994.

2.85 A.M. Khokhlov, S.E. Oran and J.C. Wheeler, A Theory of Deflagration-to-Detonation Transition in Unconfined Flames, Combustion and Flame, Vol 108, 1997, 503-517.

2.86 A.M. Khokhlov, E.S. Oran and G.O. Thomas, Numerical Simulation of Deflagration-to-Detonation Transition: The Role of Shock-Flame Interactions in Turbulent Flames, Combustion and Flame, in Press.

2.87 J.W. Dold, M. Short, J.F. Clark and N. Nikiforakis, Accumulating Sequence of Ignitions from a Propagating Pulse, Combustion and Flame, Vol. 100, 1995, 465-473.

2.88 M. Short and J.W. Dold, Corrections to Zel'dovich's <<Spontaneous Flame>> and the Onset of Detonation via Nonuniform Preheating, Dynamic Aspects of Explosion Phenomena (edited, by Kuhl A.L. et al.), Prog. In Astronautics and Aeronautics, AIAA, Vol. 154, 1993, 59-75.

2.89 A.M. Bartenev and B.E. Gelfand, Weak and Strong Ignition Within the Scope of Spontaneous Flame Concept, Twenty Fifth Symposium (International) on Combustion, The Combustion Institute, Pittsburgh, 1994, 61-64.

2.90 I. Sochet, M. Aminallah and J. Brossard, Detonability of Fuel-Oxygen and Fuel-Air Mixtures, International Journal of Shock Waves, Vol. 7, 1997, 163-174.

2.91 I. Sochet, A. Reboux and J. Brossard, Detonability of Spatially Non-Uniform Gasous Mixtures, 14th ICDERS Coimbra Portugal, Preprints II: E1.7.1-E1.7.10, 1993.

2.92 S.P. Medvedev, A.N. Polenov, S.V. Khomik and B.E. Gelfand, Initiation of Upstream-Directed Detonation Induced by the Venting of Gaseous Explosion, Twenty-Fifth

Symposium (International) on Combustion, The Combustion Institute, Pittsburgh, 1994, 73-78.

2.93 R. Blumental, K. Fieweger, K.H. Komp and G. Adomeit, Gas Dynamic Features of Self Ignition of Nondiluted Fuel/Air Mixtures at High Pressure, Combustion Science and Technology, Vol. 137, 1996, 113-114.

2.94 L. He and P. Clavin, Numerical and Analytical Studies of the Initiation of Combustion Wave by Hot Pockets, *Experimental, Modelling and Computation in Flow*, Turbulence and Combustion (ed. J. Desileri, J. Wiley), Vol. 1, 1996, 137-157.

2.95 U. Behrens, G. Langer, M. Stock and R. Wirkner, Deflagration-Detonation Transition in Hydrogen-Air-Steam Mixtures. Relevance in the Experimental Results for Real accidents Situations, Nuclear Engineering and Design, Vol. 130, 1991, 43-50.

2.96 Determination of Spontaneous Detonation (SWACER) and Flame Propagation Criteria in H_2 + Air Mixtures, Report IchP RAS @ INR FZK, 1994.

2.97 Investigation of Spontaneous Detonation Ignition Under Nonuniform Pressure and Temperature Conditions, Report IchP RAS @ INR FZK, 1993.

2.98 S.B. Dorofeev, V.P. Sidorov, M.S. Kuznetsov, I.D. Matsukov and V.I. Alekseev, Effect of Scale on the Onset of Detonations, Proc. of 17th International Colloquium on Dynamics of Explosion and Reactive Systems, Heidelberg, 1999.

2.99 G.O. Thomas, private communication 1999.

2.100 C.K. Chan and W.A. Dewit, DDT in End Gases, 27^{th} Symposium (International) on Combustion, Vol. 2, 1996, 2679.

2.101 B.E. Gelfand and S.V. Khomik, Investigation of Hydrogen + Air Fast Flame Propagation and DDT in Tube with Multidimensional Endplates, IChP RAS @INR FXK Report, 1998.

2.102 A. Veser, W. Breitung, G. Engel, G. Stern and A. Kotchourko, Deflagration-to-Detonation-Transition Experiments in Shock Tube and Obstacle Array Geometries, Report FZKA-6355, Research Center Karlsruhe, 1999.

2.103 A. Eder, C. Gerlach and F. Mayinger, Experimental Observation of Fast Deflagrations and Transition to Detonations in Hydrogen-Air Mixtures, submitted to the Symposium on Energy Engineering in the 21rst Century, Jan. 9-13, Hong Kong, 2000.

2.104 A.D Craven and D.R. Greig, The Development of Detonation OverPressures in Pipelines, Chem E Symposium Series 25, 1968, 41-50.

2.105 S.M. Kogarko, Investigation of the Pressure at the End of a Tube in Connection with Rapid Nonstationary Combustion, Soviet Physics – Technical Physics (ZhTF) 28:2041.

2.106 F. Zhang, P.A. Thibault and S. Murray, Transition from Deflagration to Detonation in Multi-Phase Slug, Combustion and Flame, Vol. 114, 1998, 13-24.

2.107 W. Breitung, S.B. Dorofeev, A.A. Efimenko, A.S. Kochurko, R. Redlinger and V.P. Sidorov, Large-Scale Experiments on Hydrogen-Air Detonation Loads and their Numerical Simulation, Proc. Int. Topl. Mtg. Advanced Reactor Safety, Pittsburgh, Pennsylvania, April 17-21, 1994, 733.

2.108 W. Breitung and R. Redlinger, A Model for Structural Response to Hydrogen Combustion Loads in Severe Accidents, Nuclear Technology, Vol. 111, 1995, 420- 425.

2.109 E. Studer and M. Petit, Use of RUT Large Scale Combustion Test Results for Reactor Applications, International Association for Structural Mechanics in Reactor Technology, 14th International Conference on Structural Mechanics in Reactor Technology, Lyon, France, 1997.

2.110 G. Ciccarelli, J.L. Boccio, T. Ginsberg, C. Finfrock, L. Gerlach, H. Tawaga and A. Malliakos, The Effect of Initial Temperature on Flame Acceleration and Deflagration-to-Detonation Transition Phenomenon, NUREG/CR-6509, May 1998.